

Sensor less DTC Using Artificial Intelligent Technique as Switching Vector Selector

Eng.Mohammed Hamouda Ali, Dr. Salama Abo-Zaid, Prof.Dr. Abd elsamia Kotb

Abstract— This paper is based on the detailed study on the characteristic of sensor less direct torque control (DTC) and output vector of the three-phase inverter, a simplified method to choose the output vector for DTC of the three-phase inverter fed induction motor is proposed. And a novel switching vector selector using the ANN (Artificial neural network) is trained under the tutor of the method mentioned above. By the usage of the ANN, when the error of the torque and stator flux is made certain, the output vector can be expediently acquired. The validity of the proposed vector selector is confirmed by the simulative results. The approach in this paper was based on the model reference adaptive control observing the rotor flux, which estimate motor mechanical speed requiring only stator quantities, the stator currents and voltages.

Index Terms— Induction Motor; Direct Torque Control; Direct Torque Neural Control; Model Reference Adaptive System Control (MRAS).

1 INTRODUCTION

The induction Motors are often termed the “Workhorse of the Industry”. This is because it is one of the most widely used motors in the world. It is used in transportation and industries, and also in household appliances, and laboratories [1]. The robustness, the low cost, the performances and the ease of maintenance make the asynchronous motor advantageous in many industrial applications or general public.

More than a decade ago, direct torque control (DTC) was introduced to give a fast and good dynamic torque response and can be considered as an alternative to the field oriented control (FOC) technique [2], [3]. The configuration is much simpler than the FOC system due to the absence of frame transformer. It also does not need pulse width modulator and position encoder, which introduces delays and requires mechanical transducers respectively. It was introduced in 1986 [2].

Direct torque control has a very fast response and simple structure which makes it to be more popular used in industrial world [4]. The key features of DTC compared to standard field oriented control includes [5]:

- No current loops so current not directly regulated.
- Coordinate transformations not required.
- No separate voltage pulse width modulator.
- Stator flux vector and torque estimation required.

2 THE BASIC PRINCIPLES OF DIRECT TORQUE CONTROL [6]

In the DTC scheme the electromagnetic torque and stator flux error signals are delivered to two hysteresis controllers as shown in Fig.1. The stator flux controller imposes the time duration of the active voltage vectors, which move the stator flux along the reference trajectory, and the torque controller determines the time duration of the zero voltage vectors, which keep the motor torque in the defined-by-hysteresis tolerance band.

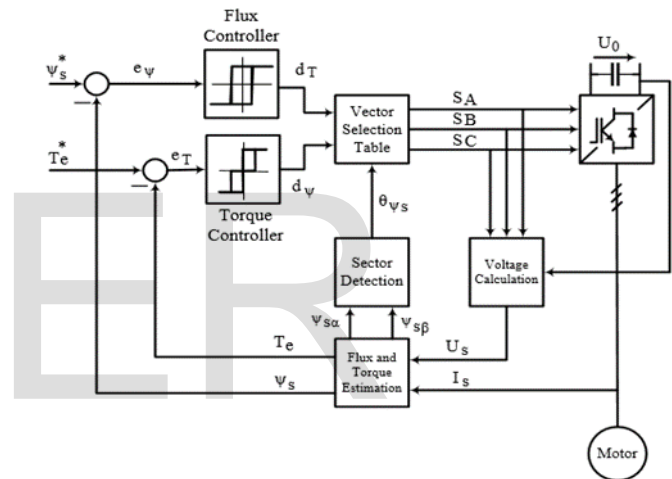


Fig.1 Block scheme of the direct torque control method

The corresponding output variables d_T , d_{ψ} and the stator flux position sector θ_{ψ_s} are used to select the appropriate voltage vector from a switching table scheme (Takahashi & Noguchi, 1986), which generates pulses to control the power switches in the inverter. At every sampling time the voltage vector selection block chooses the inverter switching state, which reduces the instantaneous flux and torque errors.

The stator flux of the induction motor can vary quickly compared to the rotor flux. DTC makes use of this property. The DTC uses two hysteresis controllers namely flux controller and torque controller to this. The control variables flux and torque are expressed in terms of stator variables. So the estimation and control of these variables becomes simple. The output of the controller determines the switch positions of the inverter which in turn accelerate or decelerate the stator flux. Hence the torque is changed at faster rate. At the same time flux controller tries to keep the operating flux around the reference value [7].

In practice the hysteresis controllers are digitally implemented. This means that they function within discrete time T_s . Consequently, the control of whether the torque or the flux is within the tolerance limits, often delays depending on the duration of the sampling period. This results in large ripples in the torque and the current of the motor.

The undesirable ripples in the electromagnetic quantities appear when the control of the values of the torque and the flux takes place at times when their values are near the allowed limits. This means that a voltage vector will be chosen which will continue to modify these quantities in a time T_s , even though these limits have been practically achieved. Accordingly, in the next control which will be carried out after time T_s , these quantities will be quite different from the desirable values. Another reason why the electromagnetic torque of the motor presents undesirable ripples is the position of the $\bar{\Psi}_s$ in each of the six sectors of its transition. In general, an undesired ripple of the torque is observed when the $\bar{\Psi}_s$ moves towards the limits of the cyclic sectors and generally during the sectors' change. Furthermore, the torque ripple does not depend solely on the systems conditions but also on the position of $\bar{\Psi}_s$ in the sector as well.

3 VECTOR MODEL OF INVERTER OUTPUT VOLTAGE [8]

In a voltage fed three phases, the switching commands of each inverter leg are complementary. So for each leg a logic state C_i ($i=a, b, c$) can be defined. C_i is 1 if the upper switch is commanded to be closed and 0 if the lower one is commanded to be close.

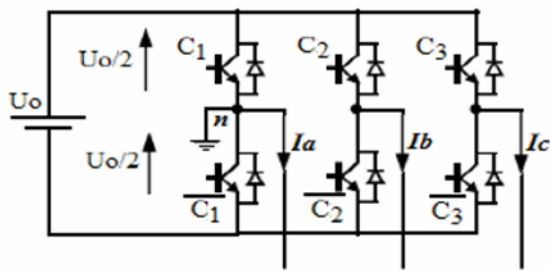


Fig.2 Three phase voltage inverter

Since there are three independent legs there will be eight different states, so eight different voltages. Applying the vector transformation described as:

$$v_s = \sqrt{\frac{2}{3}} U_0 [C_1 + C_2 e^{j\frac{2\pi}{3}} + C_3 e^{j\frac{4\pi}{3}}] \quad (1)$$

Where: U_0 is the dc voltage.

As it can be seen from the above equation, there are six nonzero voltage vectors and two zero voltage vectors which correspond to $(C1, C2, C3) = (111)/ (000)$ as shown by Figure.3. [2] [9].

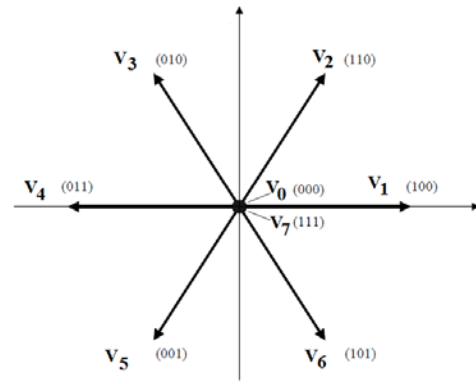


Fig.3 Available stator voltage vectors.

4 PRINCIPLES OF SWITCHING TABLE

The main concept for employing a switching table in DTC is that the estimated values of stator flux and electromagnetic torque are compared to reference values, i.e. Fig.5 $\bar{\Psi}_s^*$ and T_e^* through what is called hysteresis controller shown in Fig.4. These two hysteresis controllers are different for torque and flux. Because the flux and torque have to fall into a certain band for switching table DTC, we have two limits, which is considered as the tolerance number of allowing being "how far" from the desired value we can employ this method and still be accurate. In practice, the flux controller provides two cases (a two level controller). In contrast to achieve the desired output torque the hysteretic controller need provide three separate cases. The equations 2 and 3 represent the hysteresis band limits for the flux tables and equations 4 through 6 represent the three levels hysteresis bands of the torque tables [10].

The output signals d_ψ, d_T are defined as:

- $d_\psi = 1$, for $e_\psi > H_\psi$ (2)
- $d_\psi = 0$, for $e_\psi < H_\psi$ (3)
- $d_T = 1$, for $e_T > H_T$ (4)
- $d_T = 0$, for $e_T = 0$ (5)
- $d_T = -1$, for $e_T < H_T$ (6)

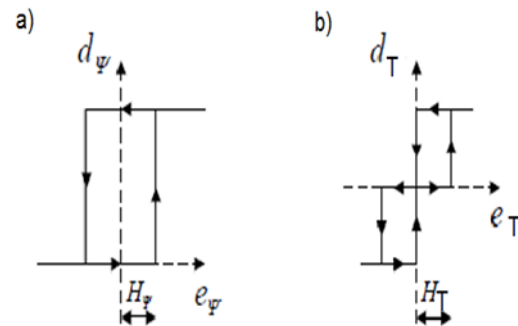


Fig.4 The hysteresis controllers a) two-level, b) three-level

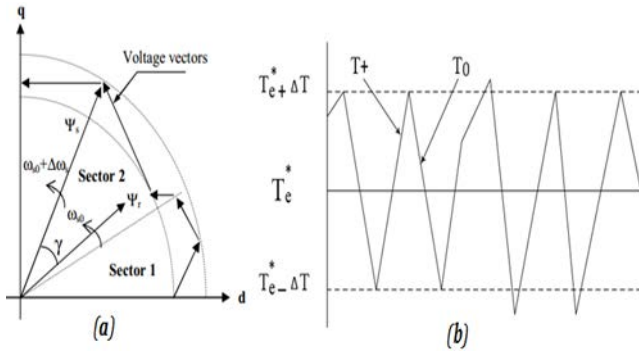


Fig.5 (a)The hysteresis band controls the stator flux voltage, (b): The torque is controlled by the three level hysteresis bands.

Where $2H_\psi$ is the flux tolerance band and $2H_T$ is the torque tolerance band. Table 1 represents the switching table logic based on the equations 2 to 6. This results in the six sectors of the hysteretic table below for inverter outputs.

TABLE I. 1.The switching table logic

\bar{V}_s	Increase	Decrease
$ \bar{\psi}_s $	\bar{V}_k, \bar{V}_{k+1} or \bar{V}_{k-1}	$\bar{V}_{k+2}, \bar{V}_{k-2}$ or \bar{V}_{k+3}
T_e	\bar{V}_{k+1} or \bar{V}_{k+2}	\bar{V}_{k-1} or \bar{V}_{k-2}

The Conventional DTC and its six sectors proposed by I. Takahashi and T. Noguchi [2].

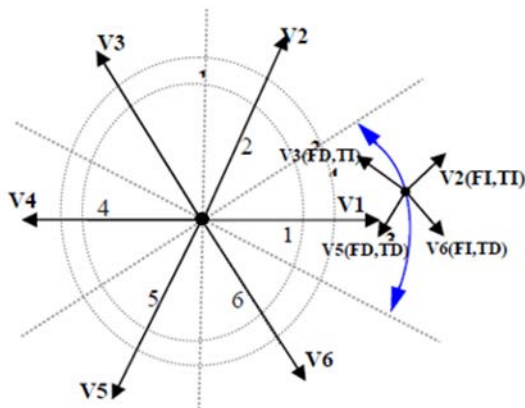


Fig.6 Conventional DTC and its six sectors

The switching selection table for stator flux vector lying in the first sector of the d-q plane as shown by figure 6 is given in Table.2 [2], [11].

TABLE I. 2.switching table for Conventional DTC

Sector		1	2	3	4	5	6
Flux	Torque						
$\Delta\psi = 1$	$\Delta T = 1$	V_2	V_3	V_4	V_5	V_6	V_1
	$\Delta T = 0$	V_7	V_0	V_7	V_0	V_7	V_0
	$\Delta T = -1$	V_6	V_1	V_2	V_3	V_4	V_5
$\Delta\psi = 0$	$\Delta T = 1$	V_3	V_4	V_5	V_6	V_1	V_2
	$\Delta T = 0$	V_0	V_7	V_0	V_7	V_0	V_7
	$\Delta T = -1$	V_5	V_6	V_1	V_2	V_3	V_4

5 STATOR FLUX LINKAGE AND TORQUE CONTROL [4]

When the proper inverter voltage sequence ($V_1 - V_6$) is selected, the stator flux is going to be rotating at the desired synchronous speed within the specified band. As mentioned earlier, the stator flux monotonically follows the stator voltage, when the stator resistance is small enough to be neglected. Thus, changing the stator flux space vector can be accomplished by changing the stator voltage during a desired period of time.

$$V_s = \frac{d\psi_s}{dt} \rightarrow d\psi_s = V_s dt \tag{7}$$

$$\Delta\psi_s = V_s \Delta t \tag{8}$$

Where $\Delta t = T_s$, is the sampling period.

We can obtain the electromagnetic flux using and the electromagnetic torque depends on the sin of the angle between the stator flux and rotor flux, i.e. θ_{sr} , as $\theta_{sr} = \theta_s - \theta_r$. Since it is easier to adjust the stator flux through the stator voltage, the variation of the developed electromagnetic torque is done by varying the stator flux vector, the stator flux magnitude and the angle between stator flux and rotor flux because the rotor flux is slowly moving but the stator flux can be changed immediately.

$$T_e = \frac{3p L_m}{2L_s} \psi_s \psi_r \sin \theta_{sr} \tag{9}$$

Where P, is the number of poles
Therefore, angle θ_{sr} as well as torque can be changed thanks to the appropriate selection of voltage vector.

$$\Delta T_e = \frac{3 P I_m}{2 L_s} (\psi_s + \Delta \psi_s) \psi_r \sin \Delta \theta_{sr} \quad (10)$$

The analysis performed by the optimal switching logic is based on the mathematical spatial vector relationships of stator flux, rotor flux, stator current, and stator voltage. The torque developed by the motor is proportional to the cross product of the stator flux vector ψ_s and the rotor flux vector ψ_r .

The magnitude of stator flux is normally kept as constant as possible and torque is controlled by varying the angle θ_{sr} between the stator flux vector and the rotor flux vector. This method is feasible because the rotor time constant is much larger than the stator time constant. Thus, rotor flux is relatively stable and changes quite slowly, compared to stator flux. When an increase in torque is required, the optimal switching logic selects a stator voltage vector V_k that develops a tangential pull on the stator flux vector ψ_s , tending to rotate it counter-clockwise with respect to the rotor flux vector ψ_r . The enlarged angle θ_{sr} created effectively increases the torque produced. When a decrease in torque is required, the optimal switching logic selects a zero-voltage vector, which allows both stator flux and produced torque to decay naturally. If stator flux decays below its normal lower limit the flux status output will again request an increase in stator flux. If the torque status output is still low, a new stator voltage vector V_k is selected that tends to increase stator flux while simultaneously reducing the angle θ_{sr} between the stator and rotor flux vectors.

6 STATOR FLUX AND TORQUE ESTIMATOR

Stator voltage components ($V_{s\alpha}, V_{s\beta}$) on perpendicular (α, β) axis are determined from measured values (v_0 and I_{sa} , b , c). Boolean switching controls (C1, C2, C3,) by, [2] [11]:

$$V_{s\alpha} = \sqrt{\frac{2}{3}} \cdot U_0 \cdot \left(c_1 - \frac{1}{2}(c_2 + c_3) \right) \quad (11)$$

$$V_{s\beta} = \frac{1}{\sqrt{2}} \cdot U_0 \cdot (c_2 - c_3) \quad (12)$$

And stator current components ($I_{s\alpha}, I_{s\beta}$):

$$I_{s\alpha} = \sqrt{\frac{2}{3}} \cdot I_{sa} \quad (13)$$

$$I_{s\beta} = \frac{1}{\sqrt{2}} \cdot (I_{sb} - I_{sc}) \quad (14)$$

The stator resistance can be assumed constant during a large number of converter switching periods T_e . The voltage vector applied to the induction motor remains also constant during one period T_e . The stator flux is estimated by integrat-

ing the difference between the input voltage and the voltage drop across the stator resistance as given by equations 15 and 16:

$$\overline{\psi_{s\alpha}} = \int_0^t (\overline{v_{s\alpha}} - R_s \cdot \overline{I_{s\alpha}}) dt \quad (15)$$

$$\overline{\psi_{s\beta}} = \int_0^t (\overline{v_{s\beta}} - R_s \cdot \overline{I_{s\beta}}) dt \quad (16)$$

The stator flux linkage phasor is given by:

$$|\psi_s| = \sqrt{(\psi_{s\alpha}^2 + \psi_{s\beta}^2)} \quad (17)$$

$$\theta_s = \tan^{-1} \frac{\psi_{s\beta}}{\psi_{s\alpha}} \quad (18)$$

By comparing the sign of the components stator flux ($\psi_{s\alpha}, \psi_{s\beta}$) and the amplitude of stator flux, we can localize the zone where we find the flux.

During the switching interval, each voltage vector is constant and equations 15 and 16 is then rewritten as in equation 19:

$$\psi_s(t) \approx \psi_{s0} + V_s T_e \quad (19)$$

In equation; ψ_{s0} stands for the initial stator flux condition. In fact, we have $\frac{d\psi_s}{dt} \approx V_s$.

Electromagnetic torque can be calculated from [11], [12]:

$$T_{em} = \frac{P}{2} \cdot (\psi_{s\alpha} \cdot I_{s\beta} - \psi_{s\beta} \cdot I_{s\alpha}) \quad (20)$$

Where: P is number of poles.

7 ANN BASED DIRECT TORQUE CONTROL

The neurons artificial network is a model of calculation with a conception schematically inspired by the real neurons functioning system. It constitutes an approach which gives more opportunities to approach the problems of perception, memory, learning and analysis under new angles. It is also a very promising alternative to avoid certain limitations of the classic numeric methods. Due to its parallel treatment of the information, it infers emergent properties able to resolve problems qualified in the past as complex [13]. In this paper, a neuronal controller is used to replace switching table, where the inputs are the error of flux torque and the position angle of stator flux, and the output is the impulses allowing the control of the inverter switches [14], [15], [16]. In order to generate this neuronal controller by Matlab / Simulink, we selected three linear feed-forward layers with five neurons in the first layer plus thirteen neurons at the second layer, and six neurons at the output layer, with the activation functions respectively of type 'logsig', 'tansig' and 'purelin'. The structure of the direct neuronal torque control of an asynchronous machine is illustrated below in figure 7.

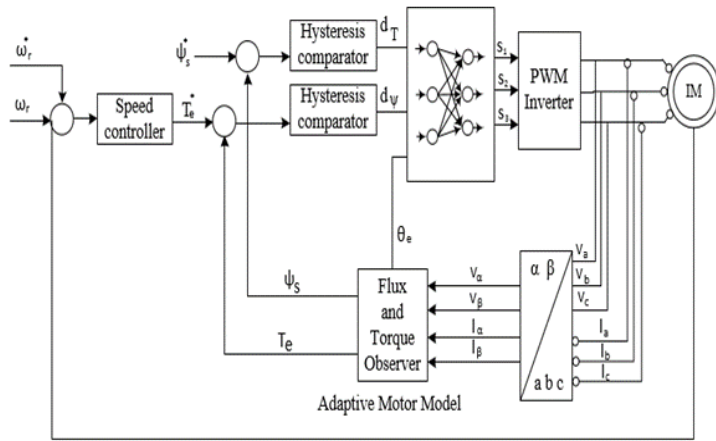


Fig.7 Direct torque neural networks controller scheme

8 MODEL REFERENCE ADAPTIVE SYSTEM (MRAS)

Sensor less drives are becoming more and more important as they can eliminate the speed sensor maintaining accurate response. Monitoring only the stator current and stator voltages, it is possible to estimate the necessary control variables. The observer type used here is a MRAS. The basic scheme of the MRAS configuration is given in figure 8. The scheme consists of two models; reference and adjustable ones and an adaptation mechanism. The block “reference model” represents voltage model which is independent of speed. The block “adjustable model” is the current model which is using speed as a parameter. The block “adaptation mechanism” estimates the unknown parameter using the error between the reference and the adjustable models and updates the adjustable model with the estimated parameter until satisfactory performance is achieved. Since the MRAS is a close-loop system, the accuracy can be increased. However, the models contain pure integrators which cause estimation error due to unknown initial condition and estimation drift due to offset in the measured currents [17], [18].

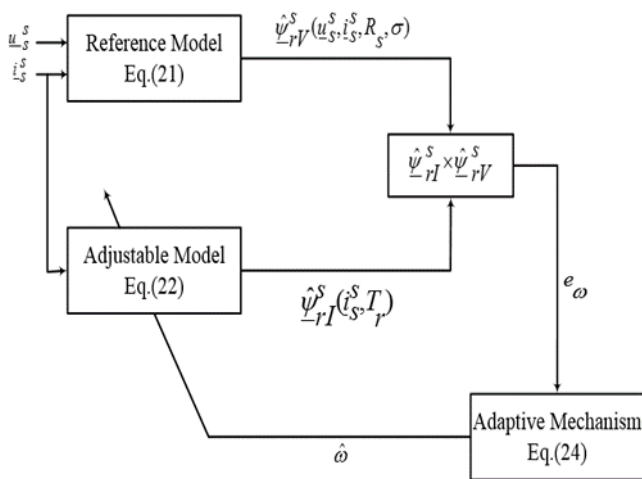


Fig.8 Conventional MRAS speed observer

8.1 Reference model

The reference rotor flux components obtained from the reference model are given by:

$$p \hat{\psi}_{rV}^s = \frac{L_r}{L_m} \left[u_s^s - (\hat{R}_s + \sigma L_s p) i_s^s \right] \tag{21}$$

8.2 Adaptive model

The rotor flux components obtained from the adaptive model are given by:

$$p \hat{\psi}_{rI}^s = \frac{L_m}{T_r} i_s^s - \left(\frac{1}{T_r} - j \hat{\omega}_r \right) \hat{\psi}_{rI}^s \tag{22}$$

8.3 Adaptation Mechanism

Finally, the adaptation scheme generates the value of the estimated speed to be used in such a way as to minimize the error between the reference and estimated fluxes. In the classical rotor flux MRAS scheme, this is performed by defining a speed tuning signal \$e_\omega\$, to be minimized by a PI controller which generates the estimated speed which is fed back to the adaptive model. The expressions for the speed tuning signal and the estimated speed can be given as:

$$e_\omega = \hat{\psi}_{rI}^s \times \hat{\psi}_{rV}^s - \hat{\psi}_{rV}^s \hat{\psi}_{rI}^s = \hat{\psi}_{rI}^s \hat{\psi}_{rV}^s - \hat{\psi}_{rV}^s \hat{\psi}_{rI}^s \tag{23}$$

$$\hat{\omega}_r = \left(K_{p\omega} + \frac{K_{I\omega}}{p} \right) e_\omega \tag{24}$$

above a symbol in equations 21 to 24 denotes estimated quantities, symbol p stands for $\frac{d}{dt}$, T_r is the rotor time constant and $\sigma = 1 - L_m^2 / (L_s L_r)$. All the parameters in the motor and the estimator are assumed to be of the same value. Undlined variables are space vectors, and sub-scripts V and I stand for the outputs of the voltage (reference) and current (adjustable) models, respectively. Voltage, current and flux are denoted with u, i and Ψ , respectively, and subscripts s and r stand for stator and rotor, respectively. Superscript s in space vector symbols denotes the stationary reference frame.

9 Simulation Model and Parameters

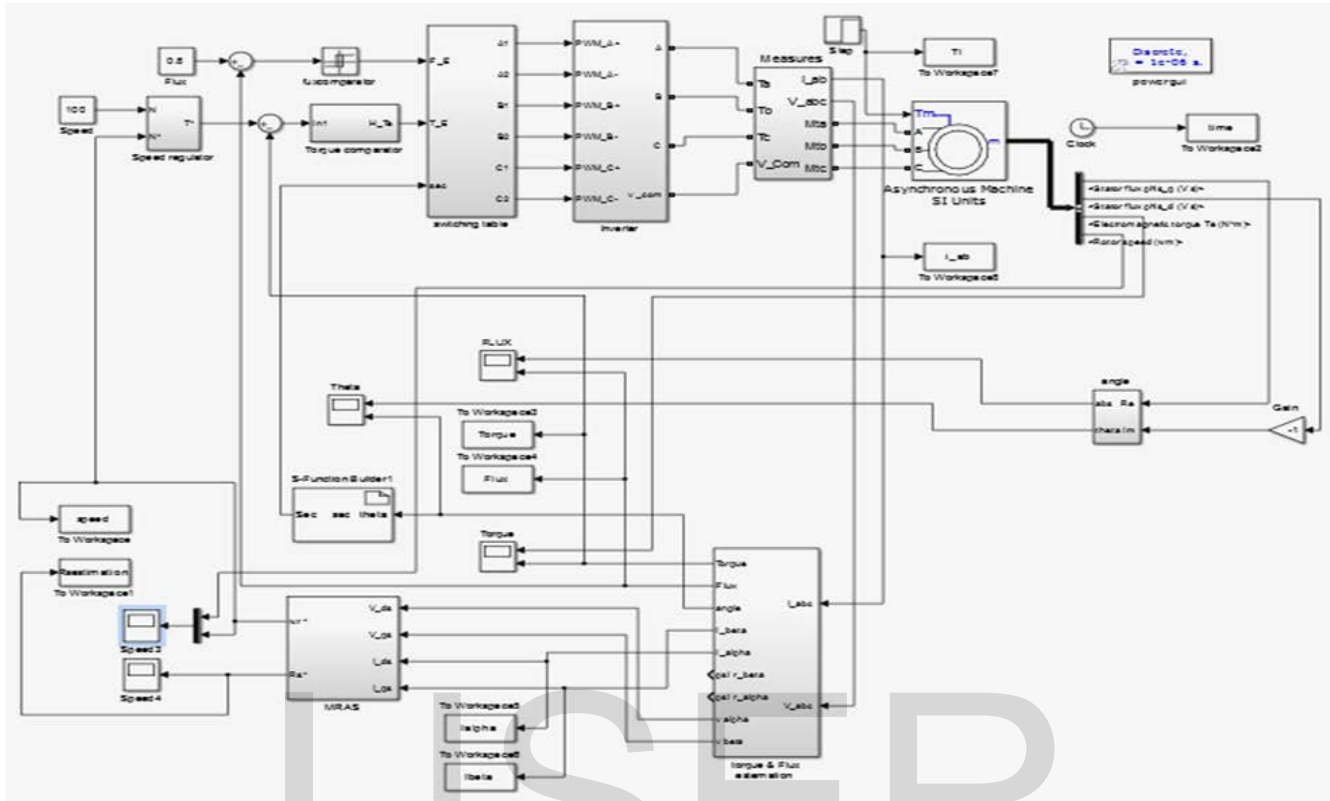


Fig.9 Simulink Model of DTC

The parameters of the induction motor are shown in table 3:

TABLE I. 3.parameters of the induction motor

Power	3hp
Stator Resistance R_s	1.115 Ω
Rotor Resistance R_r	1.083 Ω
Stator Inductance L_s	0.209674H
Rotor Inductance L_r	0.21344H
Mutual Inductance M	0.2037H
Phase Voltage V	265V
Inertia J	0.02Kgm
Frequency f	60HZ

10 SIMULATION RESULT

Conventional DTC MATLAB model was developed for 3hp induction motor at 1e-6 sec sampling time and VSI DC link voltage is 500V.

Fig. 1.

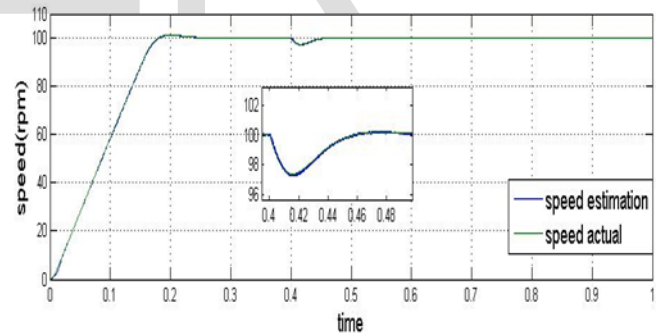


Fig.10 speed estimation against actual speed (ANN DTC).

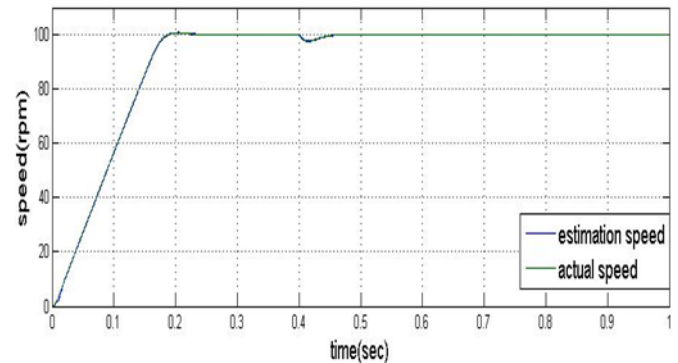


Fig.11 speed estimation against actual speed (DTC).

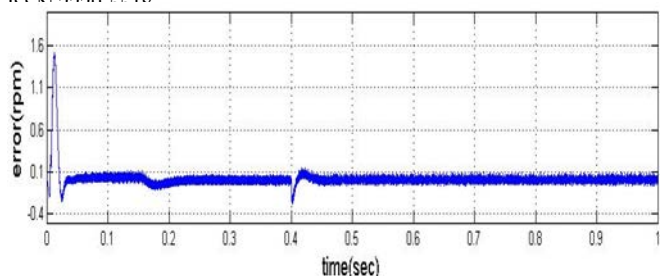


Fig.12 error on speed estimation (ANN DTC).

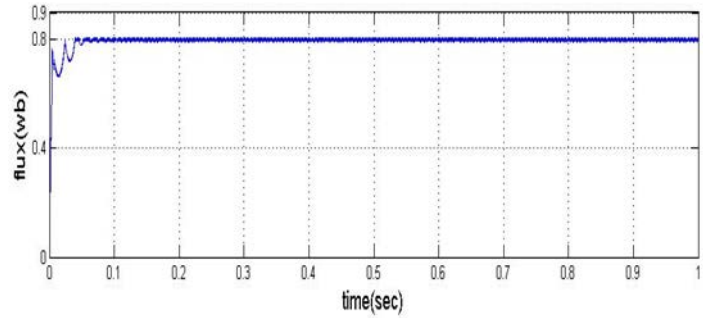


Fig.16 stator flux magnitude (ANN DTC).

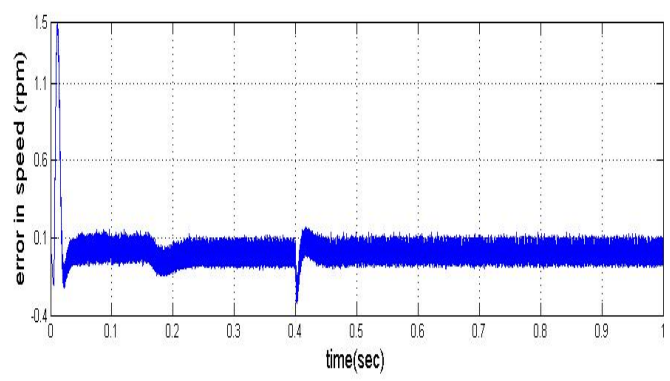


Fig.13 error on speed estimation (DTC).

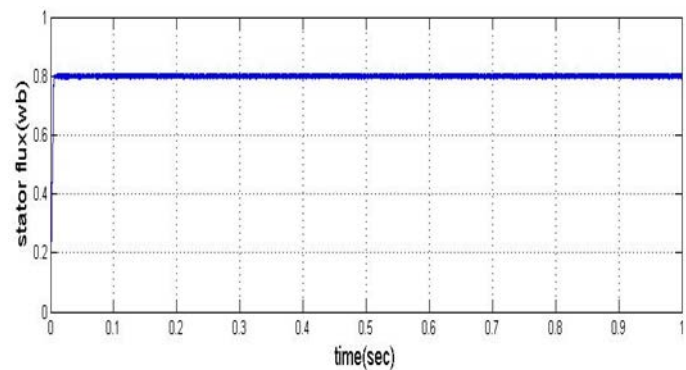


Fig.17 stator flux magnitude (DTC).

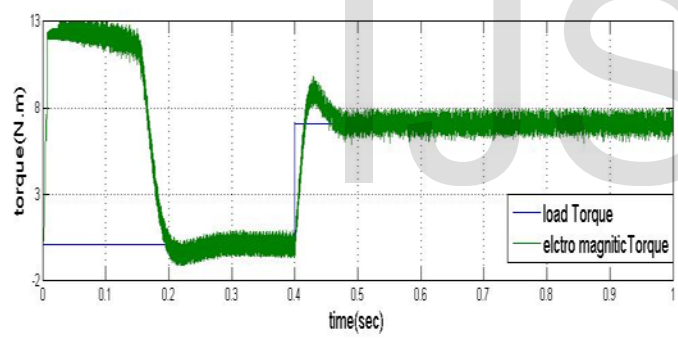


Fig.14 electromagnetic torque against the load torque (ANN DTC).

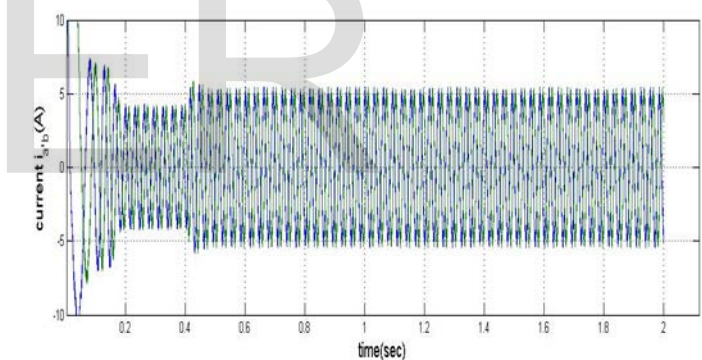


Fig.18 stator current in phase a, b (ANN DTC).

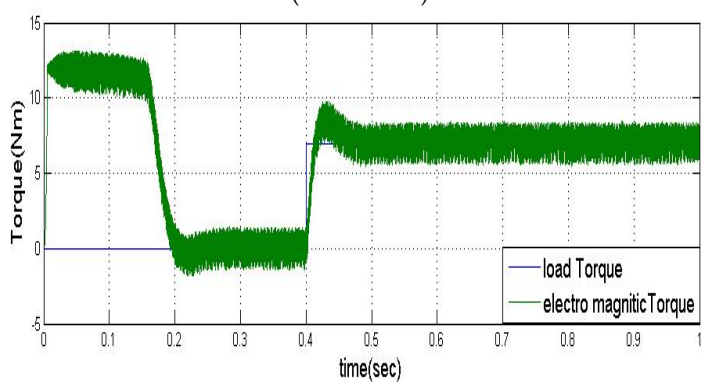


Fig.15 electromagnetic torque against the load torque (DTC).

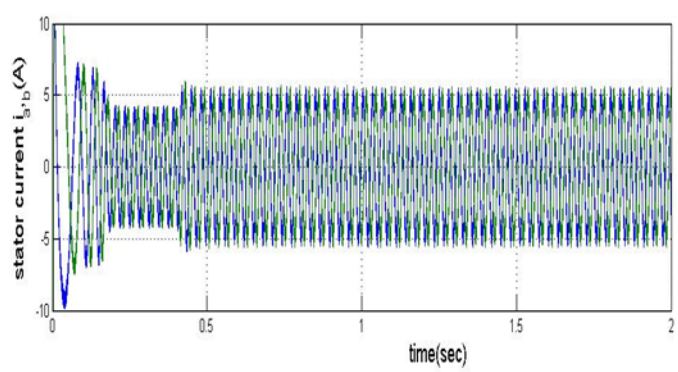


Fig.19 stator current in phase a, b (DTC).

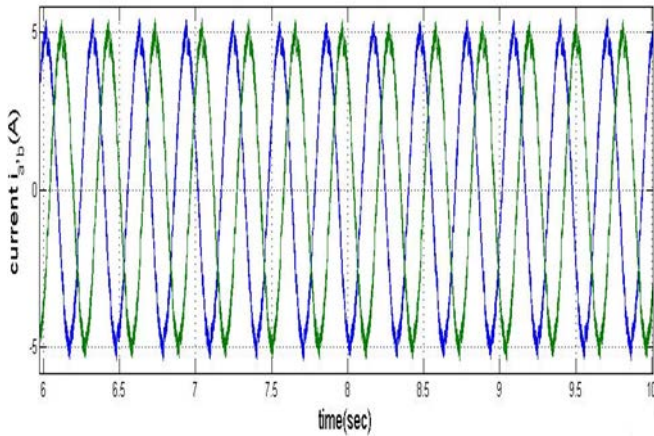


Fig.20 stator current in phase a, b at steady state (ANN DTC).

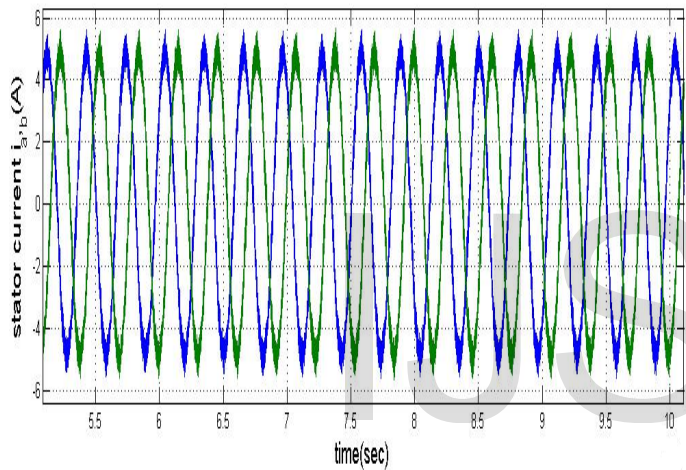


Fig.21 stator current in phase a, b at steady state (DTC).

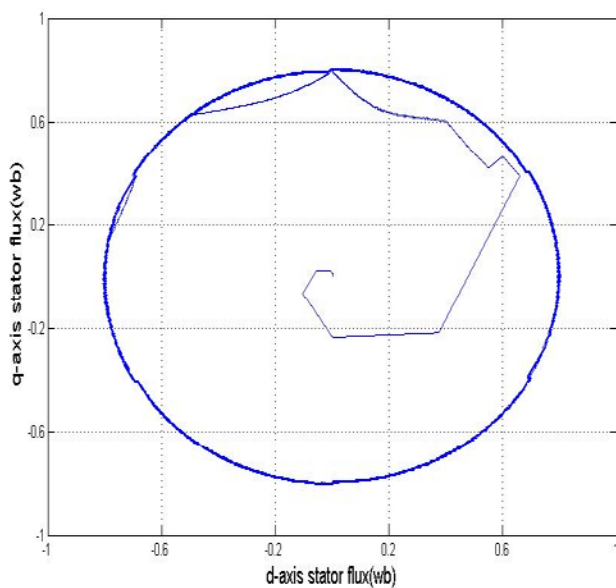


Fig.22 stator flux in d-q stationary frame (ANN DTC).

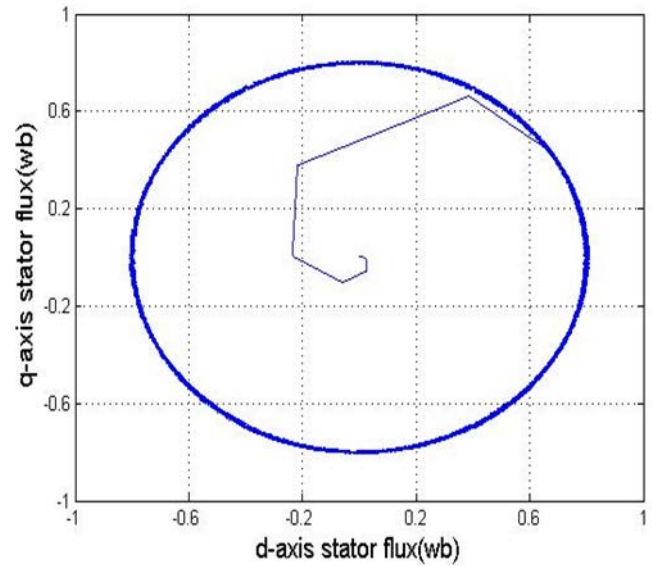


Fig.23 stator flux in d-q stationary frame (DTC).

The Induction motor speed controlling model using Conventional DTC and ANN applied DTC has been designed and studied successfully and the results of the thesis work are almost satisfying by using ANN in it as a substitution of the switching table. To compare with Conventional DTC and ANN DTC for Induction motor are simulated. The dynamic responses of speed, flux, torque and stator current for the starting process with 0 Nm load torque then 7 Nm at 0.4sec and input speed reference of 100 rpm applied are shown in Figure from 10 to 23 respectively. Figs.14 and 15 show the response of electric torque of the Conventional ANN DTC, and DTC respectively. It can be seen that the ripple in torque with ANN DTC control is less than 1Nm and with conventional direct torque control the ripple is about 3 Nm at the same operating conditions. Figs.16 and 17 show the response of stator flux magnitude of the Conventional ANN DTC and DTC respectively. By ANN DTC technique shown Fig 16, the stator flux is the fast response in transient state and the ripple in steady state is reduced remarkably compared with conventional DTC, the flux changes through big oscillation and the torque ripple is bigger in Conventional DTC. In Fig 10 and 11, It can be seen that the ripple in speed with ANN DTC is less than 0.06 rpm and with conventional direct torque control the ripple is about 1 rpm at the same operating conditions. Figs 18 and 19 show the stator current response of the ANN DTC and DTC respectively. The steady state current of the ANN DTC has negligible ripple in stator current and a nearly sinusoidal wave form while as with conventional DTC the stator current has considerably very high ripple as shown in Figs 20 and 21.

11 CONCLUSION

In this paper a conventional DTC and ANN DTC of induction

motor with estimated speed using the MRAS have been proposed. From the above the conventional direct torque control technique is used for DTC control of Induction motor. In conventional DTC method some disadvantages such as difficulties in torque and flux control at very low speed, high current and torque ripple, variable switching frequency behavior, high noise level at low speed and lack of direct current control, an adaptive torque controller must be proposed for high performance applications. So an Artificial Neural Network (ANN) control is proposed for conventional DTC scheme. The intelligent technique ANN are used for proper voltage vector selection in DTC so that the rotor speed, torque and flux performances of induction machine is improved. The conventional DTC controller compared with ANN and the results are carried out by using MATLAB/Simulink.

The main improvements shown are:

- Reduction of torque and current ripples in transient and steady state response.
- No flux droppings caused by sector changes circular trajectory.
- Operating without speed sensor.
- Good dynamic behavior and steady state responses of speed and flux even at low and high speed.

REFERENCES

- [1] Devrajee (109EE0039), Nikhar Patel (109EE0087), "V/f Control of Induction Motor Drive", Department of Electrical Engineering National Institute of Technology Rourkela-769008 (ODISHA) May-2013.
- [2] I. Takahashi, T. Noguchi, "A New Quick Response and High-Efficiency Control Strategy of an Induction Motor", IEEE Trans. Ind. Appl., vol IA-22, No 5 Sept/Oct 1986, PP.820-827.
- [3] P. Tiitinen, "The Next Generation Motor Control Method, DTC Direct Torque Control", Proc. Of Int. Conf on Power Electronics, Drives and Energy System for Industrial Growth, N. Delhi, India, pp. 37-43, 1996.
- [4] Fathalla Eldali, "A Comparative Study between Vector Control and Direct Torque Control of Induction Motor Using Matlab Simulink", Fort Collins, Colorado Fall 2012.
- [5] S Allirani and V Jagannathan, "High Performance Direct Torque Control of Induction Motor Drives Using Space Vector Modulation", IJCSI International Journal of Computer Science Issues, Vol. 7, Issue 6, November 2010.
- [6] Adamidis Georgios, and Zisis Koutsogiannis, "Direct Torque Control using Space Vector Modulation and Dynamic Performance of the Drive, via a Fuzzy Logic Controller for Speed Regulation", Democritus University of Thrace, Greece, 2011.
- [7] James N. Nash, Direct Torque Control, Induction Motor Vector Control Without an Encoder, IEEE Trans. Ind. Appl, Vol 33, March/Apr 1997 Pp 333-341.
- [8] Riad Toufouti, Salima Meziane, Hocine Benalla, "Direct Torque Control Strategy of Induction Motors", University Mentouri, Acta Electrotechnica et Informatica No. 1, Vol. 7, 2007.
- [9] Casadei, D. - Profumo, F. - Serra, G. - Tani, A: FOC - DTC: Two Viable Schemes for induction Motors Torque Control, IEEE Trans. Power Electronics. On PE, Vol.17, N°5, Sept 2002,
- [10] S. Allirani and V. Jagannathan, "High Performance Direct Torque Control of Induction Motor Drives Using Space Vector Modulation," International Journal of Computer Science, vol.7.
- [11] Depenbrock, M: Direct self - control (DSC) of inverter - fed induction machine, IEEE Trans. Power Electronics, Vol.3, N°4, Oct 1988, PP.420-829.
- [12] Toufouti, R. - Benalla, H. - Meziane S: Three- Level Inverter with Direct Torque Control For Induction Motor, World Conference on Energy for Sustainable Development: Technology Advances and Environmental Issues, Pyramisa Hotel Cairo - Egypt, 6 - 9 December 2004.
- [13] "Neural Systems for Control", ISBN: 0125264305, Elsevier Science & Technology Books, February 1997.
- [14] Luis A. Cabrera, Malik E. Elbuluk, and Donald S. Zinger, "Learning Techniques to Train Neural Networks as a State Selector for Inverter-Fed Induction Machines Using Direct Torque Control", IEEE-PE, Vol. 12, No. 5, pp 788-799, Sep, 1997, pp 788-799.
- [15] Y.V. Siva Reddy, M. Vijayakumar and T. Brahmananda Reddy, "Direct Torque Control of Induction Motor Using Sophisticated Lookup Tables Based on Neural Networks", AIML Journal, Vol.7, Issue 1, June, 2007.
- [16] R. Toufouti, S. Meziane, H. Benalla, "Direct Torque Control for Induction Motor Using Intelligent Techniques" Journal of Theoretical and Applied Information Technology, pp 35-44, JAIII, 2007.
- [17] Lotfi Baghli "Contribution à La Commande de la Machine Asynchrone, Utilisation De la logique floue, Des réseaux De Neurone et des Algorithmes Génétiques" Thèse de Doctorat en génie électrique l'université Henri Poincaré, Nancy le 14/01/1999.
- [18] C.Schauder, "Adaptive Speed Identification for Vector Control of Induction Motors Without Rotational Transducers," IEEE Trans. On Industry Applications, vol. 28, no. 5, pp. 1054-1061, 1992.